Black carbon sanitary burden in the Indo-Gangetic plain: exposures, risks and mitigation

Shubha Verma (shubha@iitkgp.ac.in)
Indian Institute of Technology Kharagpur

Sanhita Ghosh
Indian Institute of Technology Kharagpur

Olivier Boucher
Institut Pierre-Simon Laplace, Sorbonne Université/CNRS

Rong Wang
Fudan University

Laurent Menut
Ecole Polytechnique, Sorbonne Universite´ https://orcid.org/0000-0001-9776-0812

K Prasad
Indian Institute of Technology Kharagpur

Article

Keywords: black carbon, Indo-Gangetic plain, exposure

Posted Date: October 12th, 2020

DOI: https://doi.org/10.21203/rs.3.rs-75358/v1

Black carbon sanitary burden in the Indo-Gangetic plain: exposures, risks and mitigation

Shubha Verma[1,*], Sanhita Ghosh[1], Olivier Boucher[2], Rong Wang [3], Laurent Menut[4], and K Vara Prasad[1]

[1]Department of Civil Engineering, Indian Institute of Technology Kharagpur, Kharagpur-721302, India
[2]Institut Pierre-Simon Laplace, CNRS / Sorbonne Université, 75252 Paris Cedex 05, France
[3]Department of Environmental Science and Engineering, Fudan University, Shanghai, 200433
[4]Laboratoire de Météorologie Dynamique, IPSL, CNRS / Ecole Polytechnique / Sorbonne Université / Ecole Normale Supérieure, 91128 Palaiseau Cedex, France
[*]shubha@iitkgp.ac.in

ABSTRACT

A large discrepancy between simulated and observed black carbon (BC) surface concentrations over the densely populated Indo-Gangetic plain (IGP) has so far limited our ability to assess the magnitude of BC sanitary impacts in terms of population exposure, morbidity, and mortality. We evaluate these impacts using an integrated modeling framework, including a successfully predicted BC surface concentration in a high-resolution chemical transport model CHIMERE with observationally-constrained BC emissions, combined with consistent health functions for BC. Population exposure to BC is noteworthy, with more than 60 million people identified living over hotspots of BC concentration (wintertime mean $> 20\ \mu g\,m^{-3}$). A fraction of 62% of the total cardiovascular diseases mortality (CVM) burden for the megacity is found attributable to wintertime BC exposure. The semi-urban area has 50% of the CVM burden attributable to BC exposure in the total population over the IGP. More than 400 thousand lives can potentially be saved from CVM annually, by implementing prioritized emission reduction from the combustion of domestic biofuel in the semi-urban area, and diesel oil in transportation and coal in thermal power plant and brick kiln industries in megacities.

BC aerosols are mainly emitted from incomplete combustion processes, whether it is from combustion engines in the automobile sector, residential burning of wood and coal, industrial power stations using heavy oil or coal, field burning of agricultural wastes, or forest and vegetation fires[1]. Recent studies of the health effect of airborne particles provide evidence that BC is more robustly associated with health risks than bulk (non-speciated) particulate matter mass ($PM_{2.5}$ or PM_{10}), thus suggesting that BC concentration is a better indicator to consider[2–4]. BC may not be itself a toxic component of fine particulate matter (PM), but it is known to be co-emitted with toxic compounds which are byproducts of incomplete combustion of fuel and can adhere to the BC fractal morphology. BC may thus operate as a universal carrier of a wide variety of chemicals of varying toxicity into the lungs. These chemical can then come in contact with the body's major defence cells and the systemic blood circulation[3]. Recent studies also indicate health risks (per unit aerosol mass) are as much as 7–8 times larger for BC than for undifferentiated PM[2,5,6]. There is thus value in targeting specifically BC emission abatement.

Furthermore the spatial and temporal distribution of BC concentration is very heterogeneous in comparison to undifferentiated PM mass. This is attributable to a large number of local combustion sources of BC, while PM also include other species such as dust which comes in part from long-range transport over most part of the Indian subcontinent during summer season and western India during winter season[7]. This heterogeneity may lead to contrast in population exposure to BC compared to that to total PM mass. The World Health Organisation[3] suggested that BC should serve as an additional indicator to $PM_{2.5}$ to quantify human exposure to airborne pollution and assess health effects to such exposure, with consequences on how to evaluate the local or regional mitigation measures aimed to reduce population exposed to combustion aerosols.

The IGP region over the Indian subcontinent is known as one of the global hotspots of atmospheric pollutants with very large concentrations of BC aerosols in wintertime[8]. Over India, this region also has the largest population density, with area-types, e.g., from rural to megacity (refer to Table s2). Epidemiological studies provide evidence of an association between short-term exposure to elevated ambient air pollution (such as that during wintertime) and a higher risk of acute cardiovascular diseases, with systemic oxidative stress induced by air pollution as a potential underlying mechanism[4,5,9].

To estimate the magnitude of BC attributable sanitary impacts concerning population exposure, morbidity, and mortality and targeting BC emission abatement for health benefits, a conceptual plan using an integrated modeling framework as implemented in the present study is shown in Figure 1. We obtain a spatially and temporally fine resolved gridded distribution

of surface BC concentration for the wintertime over the IGP through BC transport simulation in a chemical transport model (CHIMERE). Simulating atmospheric BC concentration is indeed necessary to provide information on BC aerosols over large areas where atmospheric measurements are sparse, particularly in rural and remote locations comprising of a low population density and experiencing relatively less anthropogenic pollution than urban or megacity sites.

Evaluation of BC simulations in CHIMERE over the IGP

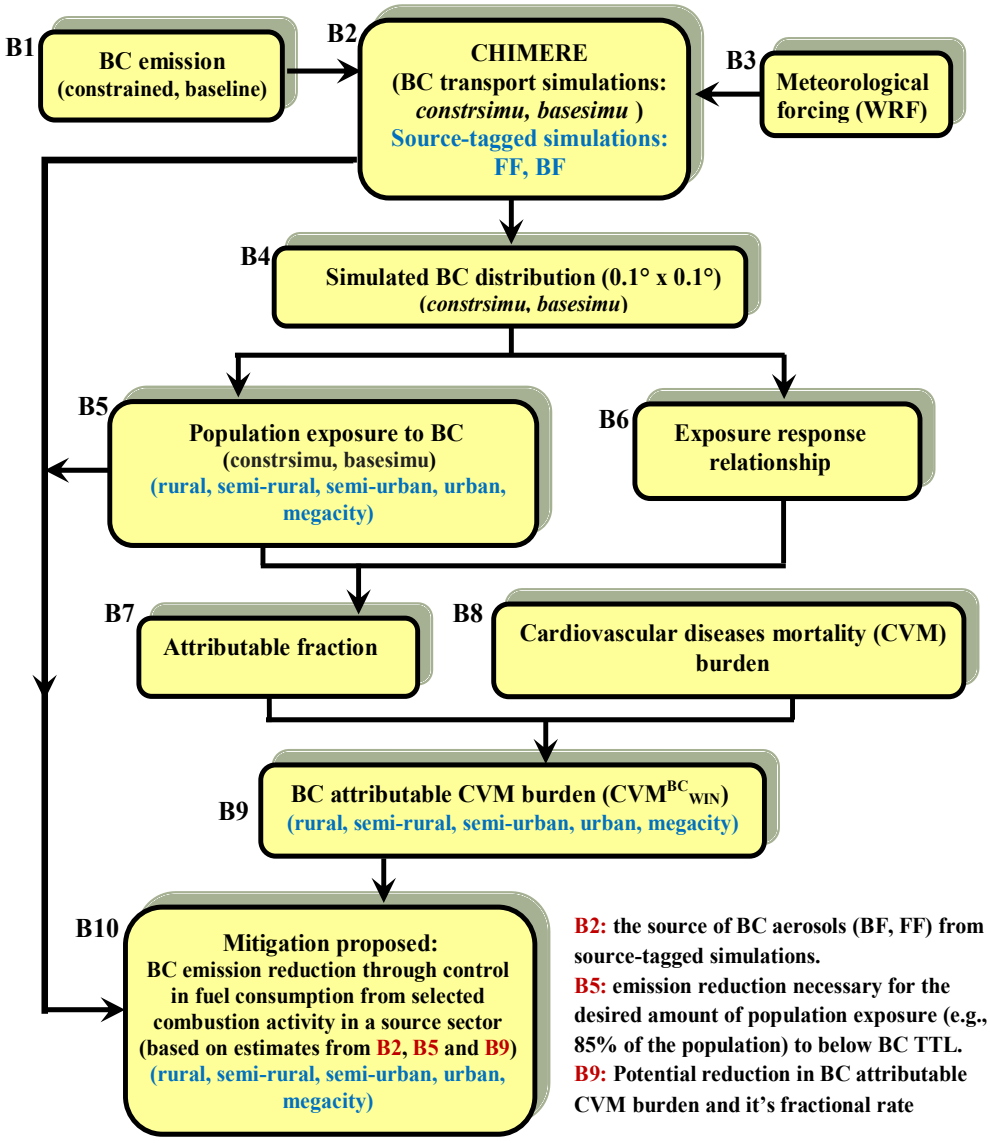

Figure 1. Flowsheet of conceptual plan to estimate the magnitude of BC attributable sanitary impacts and targeting sustainable BC emission reduction for health-benefits. The various blocks in the flowsheet are enumerated as B1, B2, B3...B10.

Two simulation experiments, *basesimu* and *constrsimu* are carried out by implementing, respectively, in CHIMERE the two emission datasets, namely, baseline BC emission and observationally-constrained BC emission (refer to 'Methods') to estimate population exposures under the scenario of simulated atmospheric BC concentration with low baseline BC emissions and that representing the present-day ambient values (close to observed) with observationally-constrained BC emissions. Spatial distribution ($0.1^\circ \times 0.1^\circ$) of BC surface concentration for all-day and daytime BC concentration averaged over the winter months (November-December) from the two simulation experiments (*constrsimu* and *basesimu*) and *constrsimu* are presented in Figures 2a–b and Figure 2c, respectively. In contrast to *basesimu* (Figure 2a), *constrsimu* (Figures 2b–c) is observed simulating adequately the BC concentration over the IGP. Patch of large wintertime BC pollution mostly comprising of wintertime

all-day (daytime) BC surface concentration in the range 14–25 (6–8) $\mu g\,m^{-3}$ is obtained from *constrsimu* estimates (Figures 2b–c) over the IGP. The feature of a large pollutant load for BC concentration over the IGP, as obtained from *constrsimu* in the present study, is found to be consistent with that exhibited for aerosol optical depth as seen from satellite-based observations (Moderate Resolution Imaging Spectroradiometer, MODIS, e.g., refer to Figure 2e-h of[10]). A comparison of the wintertime BC surface concentration (Figure 2f-g) from *constrsimu* estimates shows a good agreement with observations at stations (refer to Figure 2a–c for stations understudy) over the IGP, with the ratio of simulated to measured winter averaged all-day (daytime) concentration being near to one. The comparison from *basesimu* is also shown (Figure 2f-g) to examine the amount of reduction in atmospheric BC concentration desired compared to the measured, thereby targeting abatement in BC pollution (as discussed later) with the low baseline BC emissions. In this regard, BC surface concentration from *basesimu* is accounted for 2 to 10 times lower than its measured counterparts. The normalised mean error (NME) in *constrsimu* is 16% (14)% for both the all-day (daytime) winter averaged BC concentration (refer to Table s1 as a supplement), which lies within the uncertainty range in BC measurements (10%–20%). Unlike, the previous modeling studies which showed a large discrepancy in the simulated BC distribution in global or regional chemical transport models, with the magnitude of simulated surface BC concentrations being 4 to 9 times lower than observations, especially during winter months over the IGP[7,11–13]. Low values for the normalised mean error and root mean square error functions from *constrsimu* indicate that the combination of the CHIMERE model and observationally-constrained BC emissions could simulate BC distribution over the IGP more efficiently than reported in previous studies.

Population exposures to ambient BC concentration

In order to understand population exposures to BC (expressed as population number or relative percentage of population corresponding to area-types in the IGP exposed to a given BC concentration), the spatial distribution of population density (at a spatial resolution of $10 \times 10\,km^2$) with the overlay of contours of wintertime BC concentration for all-day and daytime mean is presented in Figures 3a and 3b, respectively. The population over the IGP is mostly spread over the semi-urban area[14] (refer to Table s2), with more than 300 million people over the IGP including, respectively, more than 150, 80, 20, and 35 million over the semi-urban, urban, megacities, and semirural areas being exposed to the wintertime all-day (daytime) mean BC concentration of magnitude mostly higher than 10 (5) $\mu g\,m^{-3}$, which is twice (just equivalent to) the BC theoretical threshold limit (TTL, refer to 'Methods'). Even more than 30 (4) million people over the rural area are also found exposed to magnitude of all-day (daytime) mean BC concentration just above the TTL. More than 60 million people live over hotspots of BC concentration (white contours in Figures 3a and 3b) zone with a typically high wintertime all-day (daytime) mean BC surface concentration larger than 20 (8) $\mu g\,m^{-3}$, i.e. comprising of values greater than 4 (1.6)-times the TTL, as identified prominently over urban areas in the eastern and northern IGP, in addition, to that over semi-urban and a few semi-rural locations. Thereby, indicating the alarming feature of BC pollutants present even for the rural/ semi-rural population belts, though, with a low population density and that with a low BC emission rate (15-times and 2–4 times lower than, respectively, megacity and semi-urban/urban belts, refer to Table s2). About 12 million people over the two megacities of the IGP (population density of $>$ 5000 people per km^{-2}) are exposed to the extreme levels of all-day (daytime) wintertime mean of BC surface concentration (as large as 40 $\mu g\,m^{-3}$ (12 $\mu g\,m^{-3}$)). The population-weighted averages (refer to Table s2) of the wintertime all-day (daytime) BC surface concentrations for the urban belt and the megacity are larger by about 3-times (1.5–1.8) and 8-times (3-times), respectively, than the rural belt.

BC concentrations from *constrsimu* and *basesimu* against the cumulative percentage of population distribution are presented in Figures 3c-h. These figures are shown considering both the overall population of the IGP (Figure 3c) and the populations corresponding to area-types over the IGP (Figures 3d-h). The cumulative distribution pattern is generally observed to exhibit an *S*-shaped curvature for all the cases examined, but a reverse curvature for the semi-urban, urban, and megacity area-types with *constrsimu* all-day mean of BC concentration. More than 85% of the population over the IGP (Figure 3c) is exposed to all-day mean BC concentration above the TTL, with about 36% being exposed to more than triple the TTL.

Analysis of the cumulative percentage population exposure for each of the area-types (Figures 3d-h) shows that more than 90% ($>$70%) of the semi-urban, urban population and megacity populations are exposed to all-day (daytime) mean BC concentration above the TTL. The exposure is really alarming as this corresponds to 70% of semi-urban and urban population being exposed to all-day mean BC concentration of value greater than 2–4 times the TTL, and specifically, that to 94% of the megacity being greater than 4-times the TTL. The BC exposure level is distressing for the semi-rural and rural population as well, with about 79% and 43%, respectively, of their population being exposed to all-day mean of BC surface concentration above the TTL. The BC exposure for the population corresponding to these area-types, though, appears to be better considering the daytime mean than the all-day mean, with about 90% of the rural and 70% of the semi-rural population being exposed to daytime mean BC concentration of value within the TTL. The population exposure for all area types, except megacities, is found to be relatively acceptable with the *basesimu* experiment, for which more than 85% of population is exposed to BC concentration below the TTL.

Thus, the above analyses indicate the extent of reduction (by a factor of 8 or by 87%) in the present-day BC emissions (as perceived from observationally-constrained BC emission data), which is required to make it equivalent to the low emission scenario from the *basesimu*. This reduction is necessary to bring about 85% of the population exposure to ambient BC levels of value below the TTL.

BC attributable cardiovascular diseases mortality (CVM) burden and potential mitigation measures

We further evaluate the health functions over the IGP as estimated in the present study (using formulation and assumption given in 'Methods') for the cardiovascular diseases mortality (CVM) attributable to wintertime BC exposure. The spatial distribution of relative risk factor (RR) (Figure 4a) indicates this being greater than one over the entire IGP, thereby indicating wintertime BC exposures being a potential risk factor over the entire IGP, including semi-rural and rural areas. Notably, RR is less than one over the rural area covering the parts of central India. The RR value is notably large (1.5 to 4) over the identified BC hotspot locations, with this being the largest for the megacities, Delhi and Kolkata (3 to 4), thereby, indicating the highest potential of BC exposure as a risk factor for the megacities. Spatial distribution of CVM attributed to the wintertime BC exposure (CVM_{BC}^{WIN}) for each gridmesh (10×10 km^2 resolution), is presented in Figure 4b. Patches of a large burden of CVM_{BC}^{WIN} (> 100 inhabitants mortality per gridmesh) is found spatially distributed over the BC hotspot locations, with the highest burden (> 500 to 1000 inhabitants mortality per gridmesh) observed in and around megacities (Kolkata and Delhi).

The CVM_{BC}^{WIN} is estimated comprising of 400 thousand deaths annually over the entire IGP. Of the total CVM_{BC}^{WIN} over the IGP, the largest fraction (49%) exists for the semi-urban area (as it has the largest population exposures to BC concentration above the TTL, refer to Table s2), followed by the urban (28%) and megacity (14%), with the lowest being for the rural (2%), followed by semi-rural (8%). Further, it is noted that CVM_{BC}^{WIN} is 22% of the total annual CVM over the IGP. In other words, a fraction of 22% of the annual mortality due to cardiovascular diseases in the total population over the IGP is attributable to wintertime BC exposure. This fraction when estimated corresponding to the classified domains or area-types (refer to Table s2) is obtained as 62% for the megacity, which is significantly high compared to that as 30% for the urban, 20% for the semi-urban, and 3% for the rural. The above analysis thus indicates an urgent requirement of the domain-wise sustainable mitigation plan towards the reduction in the combustion PM (BC) to provide health benefits to inhabitants from BC pollution exposure. The domain-wise targeted mitigation plan is suggested because the potential emission source of atmospheric BC aerosols are distinctive for the domains (e.g., for the semi-urban and urban/megacity), as discussed later in the text.

The uncertainty in CVM_{BC}^{WIN} is estimated to be about 48% (based on uncertainty in β, simulated BC concentration and mortality rate (y_0) as mentioned in 'Methods'), which is mainly due to the lack of information on β value for the Indian region. Epidemiological studies, including population exposed to various ambient levels of BC concentration, is required on a regional basis to assess more accurately the CVM_{BC}^{WIN}. Nevertheless, the relative fraction (%) of CVM_{BC}^{WIN} and that its relative distribution across the area-types over the IGP as estimated in the present study, is believed to be reasonably consistent.

In order to evaluate the domain-wise mitigation measures, we examine the source of BC aerosols over the IGP through an analysis of source-tagged simulation (refer to Figures 2d-e). Wintertime BC concentration is primarily (50%–70%) from emissions of biofuel combustion for cooking and heating in residential household sector over the eastern IGP, and that almost equally (40–50% each) from biofuel combustion in residential and fossil fuel combustion in industrial and transportation sectors over the central part of the IGP. On the other hand, wintertime BC concentration is mainly (50%–70%) from BC emissions of FF combustion over the northern IGP (in and around Delhi and the hotspots) and that over the urban area and hotspots of the eastern India (in and around Kolkata). The origin of ambient BC aerosols primarily from the FF combustion over Delhi-National Capital Region as observed in the present study, is the reason for the failure to attain the desirable level of ambient PM concentration in a recent study for highly polluted areas (e.g., Delhi) even when considering the hypothesized sensitivity experiment using the complete abatement of residential BF combustion[15]. This further justifies the usage of BC as a better indicator towards local or regional mitigation measures aimed at reducing population exposure to combustion PM, specifically over the Indian subcontinent.

In principle, 100% or so mitigation of combustion activities contributing to BC aerosols is strongly recommended. However, for sustainable attainment of health benefits, we suggest stagewise mitigation measures, to achieve 87% reduction in BC emissions, foremostly, which is required to bring more than 85% of the population exposed to the BC concentration below the TTL (based on our analysis of population exposure as discussed in 'Population exposures to ambient BC concentration'). The strategic mitigation measures, conceptualised domain-wise, e.g., for the semi-urban, urban, and megacity (refer to Figure 3i), based on prevalent emission sources of BC aerosol, and estimates of population exposures over the domain, in conjunction with that on total number and fraction of population affected from CVM attributable to wintertime BC exposure (also refer to Figure 1), is believed to be leading to sustainable achievement of potential health benefits. These measures, e.g. (i) mitigation of residential BF combustion activity over the entire IGP, preferentially, identifying the population using fuel wood and cropwaste (based on emission composition of BF combustion source, refer to 'Methods') would lead to decreasing the CVM burden to a wider extent, saving about 220 thousand lives from CVM_{BC}^{WIN} (benefitting a large number of semi-urban inhabitants

spread over a wide area of the IGP, including rural and semi-rural). The CVM burden would decrease at a large fractional rate (saving 50 thousand lives from CVM_{BC}^{WIN} out of 80 thousand lives under CVM burden for megacity) and that at a wider extent, saving 160 thousand lives from CVM_{BC}^{WIN} (out of total of 400 thousand deaths corresponding to CVM_{BC}^{WIN} over the entire IGP), through, specifically targeting urban/megacity for the (ii) reduction of FF combustion sources, preferentially of diesel oil combustion in transportation, and coal combustion in industries. As per the above suggested measures, to achieve 87% reduction in the latest BC emissions (constrained) from FF combustion source for urban/megacity, amount of BC emissions required to be reduced from diesel combustion in heavy duty vehicles, and that from coal combustion in thermal power plant (TPP) and brick kiln industries is shown in Figure 3i. This reduction corresponds to a 7-fold decrease in the diesel consumption per km^2 for urban and megacity, planned either by reducing the number of vehicles or curbing the amount of diesel consumed per vehicle (e.g., through switching to hybrid technology measures) by 85% (i.e., 530 kg vehicle^{-1} yr^{-1} to 80 kg vehicle^{-1} yr^{-1}). Further, the above reduction corresponds to a 10-fold decrease in the total coal consumption in TPP sector, or coal combustion per unit MW of electricity generated in TPP by 90% (i.e., 160 tonne MW^{-1} yr^{-1} to 16 tonne MW^{-1} yr^{-1}). The above reduction also corresponds to a 17- and 10-fold decrease in the total coal consumption in brick kilns sector, respectively, for megacity and urban regions or that to 90% decrease in coal consumption per 1000 bricks produced in the brick kiln (i.e., 300 g to 33 g of coal per 1000 bricks produced). To achieve 87% reduction in the present-day BC emissions (observationally-constrained) from BF combustion source in the semi-urban area, amount of BC emissions required to be reduced from the combustion of fuel wood, crop waste and dung cake in the residential household fuel use is shown in Figure 3i. This reduction corresponds to a 10-fold decrease in the consumption of the BF per km^2 over the IGP.

The recently launched national mission, such as Ujjawal Bharat mission of the Government of India, which promotes and aids providing clean energy combustion source preventing the residential coal and biomass fuels combustion for residential cooking, is believed would be effective in reducing the mortality risks associated with the combustion PM over the IGP. Regulatory measures are also required for curbing BC emissions from FF combustion source over the megacity and urban areas as per the above suggested measures. We suggest promoting domain-wise mitigation plans based on estimating the source-wise BC emission reduction credits and the exchange of credits among the potential source sectors which contribute to BC emissions on a regional to national to global scale. Evaluation of these plans over the Indian region is under progress and will be presented in a future study.

Conclusion

In the present study, we assess the sanitary impacts attributable to BC exposure in terms of population exposures and disease burden (cardiovascular disease mortality, CVM) for the South Asia Indo-Gangetic Plain (IGP) using an integrated modeling framework. The assessment includes using a simulated spatial distribution of BC surface concentration obtained from a high-resolution chemical transport model (CHIMERE) and comparing favorably with observations. The efficacy of CHIMERE to simulate the observed very large concentrations of BC aerosol during the wintertime with low values for the normalized mean error and root mean square error functions, is due to the implementation of an observationally-constrained BC emission dataset for the Indian region.

Population exposure to BC is remarkably high for more than three hundred million persons living in the IGP including 94% of the megacity and 70% of semi-urban/urban inhabitants being exposed to an all-day mean BC concentration of magnitude twice larger than the defined theoretical threshold limit (TTL) based on available epidemiological information (5 μg m^{-3}). These are also inferred being distressing for rural and semi-rural populations, with about 79% and 43%, respectively, of these populations estimated to be exposed to all-day wintertime mean of BC surface concentration above the TTL. The population-weighted averages of the simulated wintertime BC concentration are larger by factors 4 and 6-8, respectively, for the urban areas and megacities than the rural areas.

The spatial mapping of the relative risk factor and CVM burden attributable to BC exposure (CVM_{BC}^{WIN}) implies that all populations living in the IGP, including those in rural areas, are under the risk of BC-attributable health effects. The CVM_{BC}^{WIN} per 10×10 km^2, including more than a hundred deaths over the BC hotspot locations and as large as thousand deaths for the megacities of Kolkata and Delhi is identified in the IGP. The fraction of CVM_{BC}^{WIN} is 22% of the CVM in the total population over the IGP. Among the different area types, this fraction is the largest for the two megacities (62%), or three times that for semi-urban areas.

Based on our estimates of population exposures, an 87% reduction in present-day BC emissions is required to avoid the adversity of BC-attributable sanitary impacts and save about 400 thousand lives annually from CVM over the IGP. Health benefits from the sanitary impacts of BC are potentially attainable reducing the CVM burden by a wider extent, thereby, saving about 220 thousand lives of semi-urban including rural population from CVM_{BC}^{WIN} through the preferential mitigation of the residential fuelwood and crop-waste combustion. But, the CVM burden is estimated decreasing by a large fractional rate, saving about 50 thousand lives of megacity population (out of the CVM burden of 80 thousand lives), and by a wider extent saving about 160 thousand lives of urban/ megacity population, through the preferential reduction of diesel oil combustion

in transportation, and coal combustion in industries, specifically thermal power plants (TPP) and brick kilns. The domain-wise mitigation plan comprising of the amount of mitigation of emissions required through the corresponding reduction in fuel consumption for energy from identified combustion activity, including the total coal consumption in the industry or consumption per unit MW of electricity generated in TPP, or per 1000 of bricks produced in brick kiln industry, the diesel consumption per vehicle in the transportation, biofuel use per km^2 in the residential household sector is suggested and presented in the study.

Methods

Available studies indicated that the most likely reasons for the discrepancy between model and observations include an underestimation of BC emissions used as input, inadequate meteorology and representation of aerosol treatment, and too coarse spatial resolution in the model[7,11,16–19]. In a recent study[20], an improvement in model performance relative to observations over the East and South Asia regions was shown with a high-resolution chemical transport model, revealing an overlap of high BC exposure concentration and population density. Thereby, indicating that the inadequate BC distribution would lead to the dilution of the population exposure and the reduction of population-weighted concentration. A better agreement between model simulated and observed magnitude of atmospheric aerosol species was, however, delivered over the Indian region in a recent study using the constrained aerosol simulation approach[7,16]. Further, the constrained BC emissions were estimated over the Indian region constraining the simulated BC concentration in a general circulation model (Laboratoire de Météorologie Dynamique atmospheric General Circulation Model (LMDZT-GCM)) with the observed BC (observationally-constrained BC emissions) by combining forward and receptor modelling approaches[12].

In the present study, we implement (Figure 1) the recently estimated spatially and temporally resolved observationally-constrained BC emissions over the Indian region in a chemical transport model (CHIMERE). The efficacy of the high-resolution ($0.1^\circ \times 0.1^\circ$) CHIMERE model is evaluated based on its adequacy to simulate the observed wintertime BC distribution, comparing model estimated value with observations at stations over the IGP. The validated model BC distributions are further utilised to assess its implication to sanitary impacts of BC pollution estimating population exposures to ambient BC aerosol, and disease burden (cardiovascular diseases mortality, CVM) attributed to wintertime BC exposure. Further, it is also interesting to examine the prominent emission source of BC aerosols from source-tagged BC simulation and the extent of reasonably sustainable mitigation of BC emissions required for potential health benefits to the population living in different area-types over the IGP, e.g., from rural locations to megacities.

Simulation of BC surface concentration

Simulation of surface concentration of black carbon (BC) aerosol is carried out using two state of the art regional deterministic models: WRF v3 for the meteorology and CHIMERE v2014b for the chemistry-transport[21]. CHIMERE being in offline mode, it is forced by WRF meteorological fields. The two models are running at the same fine grid horizontal resolution of 10×10 km^2 and over the same domain of the IGP (20°N-31°N 75°E-89.4°E, refer to Figure 2a–c). The simulation is performed for the year of 2015 with a spin-up time of 10-days and analysed in the present study averaged for the winter months of November and December.

The WRF meteorological model

The WRF model is a state-of-the-art numerical weather forecast and atmospheric simulation system designed for both research and operational applications (http://www.mmm.ucar.edu/wrf/users/downloads.html). The initial and boundary meteorological conditions for WRF simulation are obtained from Global Forecast System (GFS)[22] National Center for Environmental Prediction - FINAL (NCEP-FNL) operational global analysis data at a spatial resolution of $1^\circ \times 1^\circ$. Meteorological fields are extracted from WRF at the temporal resolution of one-hour and the horizontal resolution of 10×10 km^2 (same as that for CHIMERE simulation). The characteristics of the land surface such as soil type, vegetation index, albedo or surface topography are provided by the National Center for Atmospheric Research (NCAR) and available at http://dss.ucar.edu/datasets/ds083.2/. The meteorological boundary conditions, including sea surface temperature, are updated every 6 hours. The physical scheme option used for WRF simulation include the scheme for the microphysics[23], subgrid convection by the Grell-3D scheme[24], the NOAH land surface module[25], the Yonsei University planetary boundary layer scheme[26], and the Rapid Radiative Transfer Model (RRTMG) for radiative transfer[27].

The CHIMERE chemistry-transport model

CHIMERE is a regional chemistry-transport model dedicated to the simulation of tens of gaseous and aerosols species,[21]. In this study the model version 2014b is used. The aerosol module in CHIMERE provides hourly concentrations of ten chemical species: sulphates, nitrates, ammonium, primary organic and black carbon (OC and BC), secondary organic aerosols (SOA), sea salt, natural and anthropogenic dust and water[28]. Aerosols are represented with ten bins, with mean mass median diameters ranging from 0.05 to 40 μm. Radiation and photolysis are calculated online using the FastJX module,[29]. Horizontal transport

is solved with the van Leer scheme,[30] and with a time-step of 10 minutes. Vertically, mixing is diagnosed from vertical velocity and diffusion follows a classical K_z approach[21]. Boundary layer height is diagnosed using the[31] scheme and deep convection fluxes are calculated using the[32] scheme. The deposition module of the model includes both wet and dry deposition processes for aerosols[33,34].

Boundary conditions are determined by monthly climatologies of global chemistry transport model LMDZT-GCM coupled to the Interactions between Aerosols and Chemistry (INCA) model[35]. Meteorological fields required by CHIMERE as input (e.g., 3-D wind, air temperature, relative humidity) are provided from those simulated at an hourly rate in the WRF model.

Anthropogenic emissions and simulation experiments

In the present study, two simulation experiments are carried out with CHIMERE. These are done by implementing in CHIMERE the two emission data sets (at a spatial resolution $0.25^\circ \times 0.25^\circ$ over India): (i) recently estimated constrained BC emission (annual BC emission rate of 2534 Gg yr^{-1}) over the Indian region[12], this experiment is termed as "*constrsimu*", (ii) extracted baseline BC emission (annual BC emission rate of 388 Gg yr^{-1}) from those implemented for forward BC simulation in the Laboratoire de Météorologie Dynamique atmospheric General Circulation Model (LMDZT-GCM) (Verma et al., 2011) and which were obtained from the bottom-up BC emission data (of year 2000)[36,37], termed as "*basesimu*" experiment.

Besides the above-mentioned simulation experiments, a source-tagged BC simulation experiment is also carried out using constrained BC emissions in CHIMERE. This is done to examine the relative contribution of BC emission source to atmospheric BC concentration and evaluate the source-based mitigation of emissions for area-types (e.g., megacity, urban, semi-urban) over the IGP through the corresponding reduction in fuel consumption for energy from identified selected combustion activity in a source sector (Figure 1). In the source-tagged BC simulation, the BC aerosol transport and atmospheric processes are simulated, implementing BC emissions in CHIMERE for each of the source sectors, including residential biofuel (BF) and fossil fuel (FF) combustion, with emissions outside that source sector being switched off.

For the BF and FF source sectors, on estimating the relative composition (%) of BC emission from various fuel combustion activities for energy, it is seen that this composition in BF source sector comprises of BC emissions primarily from the combustion of residential fuelwood (50%) followed by that of cropwaste (20%), dung cake and forest biomass (10% each) for cooking and heating in the residential household sector. That for the FF source sector, this is mainly from the combustion of diesel oil (59%) in transportation, followed by coal combustion (40%, comprising of 23% from brick kiln industry and 17% from the thermal power plant). The above estimation includes the merging of the information on emission composition of source sector with the total constrained BC emissions, information on activity-wise BC emission factor as that used in bottom-up emissions in *basesimu*, and that on fuel consumption for combustion activity for energy from the survey data of the Government of India (GoI)[38,39], including the report from the Department of Agriculture and Cooperation, MoA, and Land records and survey report, Government of West Bengal.

Surface observations

To evaluate the efficacy of the high-resolution CHIMERE model with the implemented observationally-constrained BC emissions, BC surface concentrations from the *constrsimu* is compared with their observed counterparts obtained from available studies at sites over the IGP (refer to Table s1). The comparison includes estimating the ratio between model and observed BC (refer to Figures 2a–c)) and the statistical error, including normalized mean error (NME), and root mean square error (RMSE) for wintertime mean values (refer to Table s1). The comparison is made using daytime, and all-day values averaged over the wintertime. This is because the daytime mean BC concentration exhibits a low hourly variability and corresponds to the well-mixed layer of atmosphere[40,41]. Evaluation of model estimates for both daytime and all-day averages thus provides a systematic approach to identify the model discrepancy, if primarily due to emissions or that due to physical/chemical processes (which govern the atmospheric residence time of aerosols).

Population exposure and BC attributable disease burden over the IGP

To assess the BC attributable sanitary impacts, we estimate the population exposure to ambient BC aerosols and the burden of disease (cardiovascular diseases mortality, CVM) attributed to wintertime BC exposure. For the spatial mapping of the population exposure to ambient BC, the gridded distribution of BC surface concentration is overlaid on a population density distribution map for the IGP region. The population density distribution is available at a spatial resolution of 10×10 km^2 (same as that of the simulated BC concentration) from[14]. The spatial distribution of the wintertime mean of BC surface concentration estimated over the IGP from the *constrsimu* is further used to calculate gridded distributions of the health functions like the relative risk factor (RR), the attributable fraction (AF) and burden of disease attributed to wintertime BC exposure. Relative risk (RR) factor is the ratio of the risk of an outcome such as disease or mortality in one group (the exposed group) to that in any other group (generally the control group) (http://www.medicalbiostatistics.com/rr-or-etc.pdf). When the RR associated with an agent or a circumstance (here BC exposure) is larger than 1, then the agent is called a risk factor. When the relative risk associated with the agent is less than 1, then the agent is called a protective factor. If the relative risk equals

1, then agent is not associated with the outcome. Relative risk factor corresponding to BC exposure is calculated in each grid according to the following equation[2,42]:

$$RR = e^{\beta \Delta x} \tag{1}$$

where β is the concentration response factor (CRF), which measures the increase in the health risk per unit increase in BC concentration (Δx in $\mu g\,m^{-3}$) beyond the theoretical threshold limit (TTL, defined later). In the present study, health functions are estimated for the cardiovascular diseases mortality (CVM, i.e. the number of people in a population who die as a result of cardiovascular diseases) attributable to wintertime BC exposure. This is because the value of β is estimated based on information from epidemiological studies providing evidence of an association between daily mortality (from cardiovascular disease) and BC particles for cooler months[5]. This value is obtained as 0.0214 per $\mu g\,m^{-3}$ of BC with an uncertainty of 43% which is nearly equivalent to that provided in[2]. The focus to consider health functions associated to CVM is also consistent with the presence of a high burden of chronic respiratory diseases in India and that with the highest risk attributable to air pollution[43]. It may be noted that β is based on the information of BC concentration exposure and response for CVM from epidemiological studies performed in the USA. Due to the lack of epidemiological information over the Indian region, and taking into account that the causes of CVM would be more comparable globally than the all-cause mortality[44,45], using β for CVM from the USA-based study is a useful compromise. The health risk estimates, as obtained from equation 1 for large BC exposures is, however, found to be consistent. As it is also noted that estimates of RR due to a given BC exposure over the IGP, using the logarithmic model, equation 1, conform well, when compared to estimates of RR (for chronic obstructive pulmonary disease, COPD) due to PM exposure using integrated exposure-response (IER) model[46], the formulation of which takes into account high PM exposures in ambient environments. The comparison with IER estimates is made corresponding to 10-times of respective BC concentration, considering health risk estimates (per unit mass) are 7–8 times larger for BC than PM.

In equation 1, Δx (spatially resolved at 10×10 km^2) is estimated as:

$$\Delta x = C - C_0 \tag{2}$$

where C_0 is the theoretical threshold limit (TTL), that is the value below which there is no noticeable adverse health effects, assumed to be 5 $\mu g\,m^{-3}$ for BC exposure, and C is the wintertime mean (daytime or all-day values averaged over the winter months) BC concentration to which a given population is exposed to, at the 10×10 km^2 resolution and also expressed in $\mu g\,m^{-3}$. It may be noted that the air quality standards for PM are based on 24-hour mean mass concentration of PM measured as PM_{10} or $PM_{2.5}$ (PM with aerodynamic diameters ≤ 10 μm or 2.5 μm), which are respectively 50 and 25 $\mu g\,m^{-3}$[3]. There is no air quality standards for BC concentration, but available studies consider health effect estimates corresponding to BC as for 1 $\mu g\,m^{-3}$ of ambient BC concentration per 10 $\mu g\,m^{-3}$ of PM_{10}[2]. The TTL for BC assumed is consistent with the above consideration (i.e. one-tenth of the air quality standard for 24-hour mean mass concentration of PM_{10}). Also, the TTL considered is consistent with the average ambient BC surface concentration during clean environmental conditions (southwest monsoon season, rainy season) from observations of BC measurement in an urban location (e.g. Kolkata), which is obtained as 5 $\mu g\,m^{-3}$[41]. The TTL is also considered to be reasonable from the perspective that it is found to lie within the range of all-day mean BC concentration (2–8 $\mu g\,m^{-3}$) estimated over relatively less polluted rural area (refer to Figure 2b) during wintertime.

Further, the Attributable fraction (AF), defined as the fraction of excess CVM factor attributed to wintertime BC exposure, is estimated. The AF is calculated for each grid at the same resolution according to the following equation:

$$AF = \frac{RR - 1}{RR}. \tag{3}$$

The CVM burden attributed to the wintertime BC exposure (CVM_{BC}^{WIN}) is then estimated as:

$$CVM_{BC}^{WIN} = y_0 \times AF \times PD \times a \tag{4}$$

where y_0 is the age-standardised mortality rate (deaths per 100,000 people in a year) due to cardiovascular diseases, AF is the Attributable fraction due to wintertime BC exposure, PD is the gridded population density in unit of 100,000 people per km^2 and a is the area of the gridmesh (in km^2). The y_0 parameter is obtained from the global burden of cardiovascular diseases for the rural/semi-rural, urban/semi-urban, and megacity area-types over India as respectively 241, 360, and 414 deaths per

100,000 people in a year (2010) based on information from available studies[47,48]. The y_0 used correspond to the mortality rate due to cardiovascular diseases for rural type (Andhra Pradesh) , urban/ semi-urban (Kerala), megacity (Mumbai) as presented in above mentioned refereed studies. This estimation is shown on Figure 4b and also integrated for each of the classified area-types over the IGP (Table s2). The mortality rate due to cardiovascular diseases for the entire India was inferred as 272 deaths per 100,000 people with an uncertainty of 5%[47,48].

References

1. Bond, T. C. *et al.* Bounding the role of black carbon in the climate system: A scientific assessment. *J. Geophys. Res.* **118**, 5380–5552 (2013).

2. Janssen, N. A. *et al.* Black carbon as an additional indicator of the adverse health effects of airborne particles compared with pm10 and pm2.5. *Environ. Heal. Perspectives* **119**, 1691–1699 (2011).

3. Janssen, N. A. *et al. Health effects of black carbon* (WHO Regional Office for Europe, Denmark, 2012).

4. Li, W. *et al.* Short-term exposure to air pollution and biomarkers of oxidative stress: the Framingham Heart Study. *J. Am. Hear. Assoc.* **5**, e002742 (2016).

5. Ostro, B., Feng, W.-Y., Broadwin, R., Green, S. & Lipsett, M. The effects of components of fine particulate air pollution on mortality in california: results from calfine. *Environ. health perspectives* **115**, 13–19 (2007).

6. Smith, K. R. *et al.* Public health benefits of strategies to reduce greenhouse-gas emissions: health implications of short-lived greenhouse pollutants. *The lancet* **374**, 2091–2103 (2009).

7. Kumar, D. B., Verma, S., Boucher, O. & Wang, R. Constrained simulation of aerosol species and sources during pre-monsoon season over the Indian subcontinent. *Atmos. Res.* **214**, 91–108, DOI: https://doi.org/10.1016/j.atmosres.2018.07.001 (2018).

8. Ramanathan, V. & Carmichael, G. Global and regional climate changes due to black carbon. *Nat. Geosci.* **1**, 221–227, DOI: 10.1038/ngeo156 (2008).

9. Shah, A. S. *et al.* Short term exposure to air pollution and stroke: systematic review and meta-analysis. *bmj* **350**, h1295 (2015).

10. Pani, S. K. & Verma, S. Variability of winter and summertime aerosols over eastern India urban environment. *Atmos. Res.* **137**, 112–124 (2014).

11. Pan, X. *et al.* A multi-model evaluation of aerosols over South Asia: common problems and possible causes. *Atmos. Chem. Phys.* **15**, 5903–5928, DOI: 10.5194/acp-15-5903 (2015).

12. Verma, S., Reddy, D. M., Ghosh, S., Kumar, D. B. & Chowdhury, A. K. Estimates of spatially and temporally resolved constrained black carbon emission over the Indian region using a strategic integrated modelling approach. *Atmospheric Res.* **195**, 9–19, DOI: 10.1016/j.atmosres.2017.05.007 (2017).

13. Ajay, P., Pathak, B., Solmon, F., Bhuyan, P. K. & Giorgi, F. Obtaining best parameterization scheme of RegCM 4.4 for aerosols and chemistry simulations over the CORDEX South Asia. *Clim. Dyn.* DOI: 10.1007/s00382-018-4587-3 (2019).

14. Census. *Primary Census Abstracts* (Registrar General of India, Ministry of Home Affairs, Government of India, New Delhi-110011, 2011).

15. Chowdhury, S. *et al.* Indian annual ambient air quality standard is achievable by completely mitigating emissions from household sources. *PNAS* 1–6, DOI: 10.1073/pnas.1900888116 (2019).

16. Santra, S. *et al.* Simulations of black carbon (BC) aerosol impact over Hindu Kush Himalayan sites: validation, sources, and implications on glacier runoff. *Atmos. Chem. Phys.* **19**, 2441–2460,, DOI: https://doi.org/10.5194/acp-19-2441-2019 (2019).

17. Wang, R. *et al.* Estimation of global black carbon direct radiative forcing and its uncertainty constrained by observations. *J. Geophys. Res. Atmos.* **121**, 5948–5971, DOI: 10.1002/2015JD024326 (2016).

18. Verma, S., Venkataraman, C. & Boucher, O. Attribution of aerosol radiative forcing over India during the winter monsoon to emissions from source categories and geographical regions. *Atmos. Environ.* **45**, 4398–4407, DOI: 10.1016/j.atmosenv.2011.05.048 (2011).

19. Reddy, M. S. *et al.* GCM estimates of aerosol transport and radiative forcing during INDOEX. *J. Geophys. Res.* **109**, DOI: 10.1029/2004JD004557 (2004).

20. Wang, R. *et al.* Exposure to ambient black carbon derived from a unique inventory and high-resolution mode. *PNAS* **111**, 2459–2463 (2014).

21. Menut, L. *et al.* Chimere 2013: a model for regional atmospheric composition modelling. *Geosci. Model. Dev.* **6**, 981–1028 (2013).

22. Kalnay, E., Lord, S. J. & McPherson, R. D. Maturity of operational numerical weather prediction: Medium range. *Bull. Am. Meteorol. Soc.* **79**, 2753–2770 (1998).

23. Lin, Y. L., Farley, R. D. & Orville, H. D. Bulk parameterization of the snow field in a cloud model. *J.Climate Appl. Met.* **22**, 1065–1092 (1983).

24. Grell, G. & Devenyi, A. D. A generalized approach to parameterizing convection combining ensemble and data assimilation techniques. *Geophys. Res. Lett.* **29**, 1693, DOI: 10.1029/2002GL015311 (2002).

25. Chen, F. & Dudhia, J. Coupling an Advanced Land-Surface Hydrology Model with the Penn State-NCAR MM5 Modeling Syste. Part I: Model Implementation and Sensitivity. *Mon. Weather. Rev.* **129**, 569–585 (2001).

26. Hong, S. Y., Noh, Y. & Dudhia, J. A new vertical diffusion package with an explicit treatment of entrainment processes. *Mon. Weather. Rev.* **134**, 2318–2341 (2006).

27. Mlawer, E. J., Taubman, S. J., Brown, P. D., Iacono, M. J. & Clough, S. A. Radiative transfer for inhomogeneous atmospheres: RRTM, a validated correlated-k model for the longwave. *J. Geophys. Res.* **102**, 16663–16682 (1997).

28. Bessagnet, B. *et al.* Aerosol modeling with CHIMERE-preliminary evaluation at the continental scale. *Atmos. Environ.* **38**, 2803–2817, DOI: 10.1016/j.atmosenv.2004.02.034 (2004).

29. Wild, O., Zhu, X. & Prather, M. J. Fast-j: Accurate simulation of in- and below-cloud photolysis in tropospheric chemical models. *J. Atmos. Chem.* **37**, 245–282 (2000).

30. van Leer, B. Towards the ultimate conservative difference scheme: IV. A new approach to numerical convection. *J. Comput. Phys.* **23**, 276–299 (1979).

31. Troen, I. & Mahrt, L. A simple model of the atmospheric boundary layer: Sensitivity to surface evaporation. *Boundary-Layer Meteorol.* **37**, 129–148 (1986).

32. Tiedtke, M. A comprehensive mass flux scheme for cumulus parameterization in large-scale models. *Mon. Weath. Rev.* **107**, 1779–1800 (1989).

33. Wesely, M. Parameterization of Surface Resistances to Gaseous Dry Deposition in Regional-Scale Numerical Models. *Atmos. Environ.* **23**, 1293–1304 (1989).

34. Zhang, L., Gong, S., Padro, J. & Barrie, L. A size-segregated particle dry deposition scheme for an atmospheric aerosol module. *Atmospheric Environment* **35(3)**, 549–560 (2001).

35. Szopa, S., Foret, G., Menut, L. & Cozic, A. Impact of large scale circulation on european summer surface ozone and consequences for modelling forecast. *Atmospheric Environ.* **43**, 1189–1195 (2009).

36. Reddy, M. S. & Venkataraman, C. Inventory of aerosol and sulphur dioxide emissions from India: I - Fossil fuels combustion. *Atmos. Environ.* **36**, 677–697 (2002a).

37. Reddy, M. S. & Venkataraman, C. Inventory of aerosol and sulphur dioxide emissions from India: II - Biomass combustion. *Atmos. Environ.* **36**, 699–712 (2002b).

38. MoSPI. *Statistical Year Book* (Central Statistics Office, Ministry of Statistics and Programme Implementation, Government of India, New Delhi, 2018).

39. MoSPI. *Energy statistics* (Central Statistics Office, Ministry of Statistics and Programme Implementation, Government of India, New Delhi, 2018).

40. Verma, S., Pani, S. & Bhanja, S. Sources and radiative effects of wintertime black carbon aerosols in an urban atmosphere in east india. *Chemosphere* **90**, 260–269, DOI: 10.1016/j.chemosphere.2012.06.063 (2013).

41. Pani, S. K. & Verma, S. Variability of winter and summertime aerosols over eastern India urban environment. *Atmos. Res.* **137**, 112–124 (2014).

42. Krewski, D. *et al.* Extended follow-up and spatial analysis of the american cancer society study linking particulate air pollution and mortality. *Res. Rep. Heal. Eff. Inst.* **140** (2009).

43. Salvi, S. *et al.* The burden of chronic respiratory diseases and their heterogeneity across the states of India: the Global Burden of Disease Study 1990–2016. *Lancet Glob. Heal.* **6**, e1363–e1374 (2018).

44. Anenberg, S. C. *et al.* Impacts of global and regional and sectoral black carbon emission reductions on surface air quality and human mortality. *Atmos. Chem. Phys.* **11**, 7253–7267 (2011).

45. Lelieveld, J., Evans, J. S., Fnais, M., Giannadaki, D. & Pozzer, A. The contribution of outdoor air pollution sources to premature mortality on a global scale. *Nature* **525**, 367 (2015).

46. Burnett, R. T. *et al.* An integrated risk function for estimating the global burden of disease attributable to ambient fine particulate matter exposure. *Environ. Heal. Perspectives* **122**, 397–403, DOI: https://doi.org/10.1289/ehp.1307049 (2014).

47. Prabhakaran, D., Jeemon, P. & Roy, A. Cardiovascular diseases in India: current epidemiology and future directions. *Circulation* **133**, 1605–1620 (2016).

48. Prabhakaran, D. *et al.* The changing patterns of cardiovascular diseases and their risk factors in the states of India: the Global Burden of Disease Study 1990–2016. *The Lancet Glob. Heal.* **6**, e1339–e1351 (2018).

Acknowledgments

This work was supported through a grant received for the project National Carbonaceous Aerosol Programme–Carbonaceous Aerosol Emissions, Source Apportionment and Climate impacts (NCAP–COALESCE) from the Ministry of Environment, Forest, and Climate Change (14/10/2014-CC (Vo.II)), Govt. of India at the Indian Institute of Technology Kharagpur.

Data availability. The data in this study are available from the corresponding author upon request (shubha@iitkgp.ac.in).

Author contributions. SV planned and coordinated the study and wrote the paper. SG conducted the BC transport simulations, performed calculations of health functions, emission reduction, and produced figures. OB advised throughout the paper's preparation, analysis of results, and contributed to writing and completion of this paper. RW contributed to the writing of the paper. LM advised and checked for the technicality of the CHIMERE model configuration and contributed to the paper. SG was supported by KVP's contribution to calculations and model setup and help in the literature review in initiating this paper. All authors contributed to the manuscript.

Competing interests. The authors declare that they have no conflict of interest.

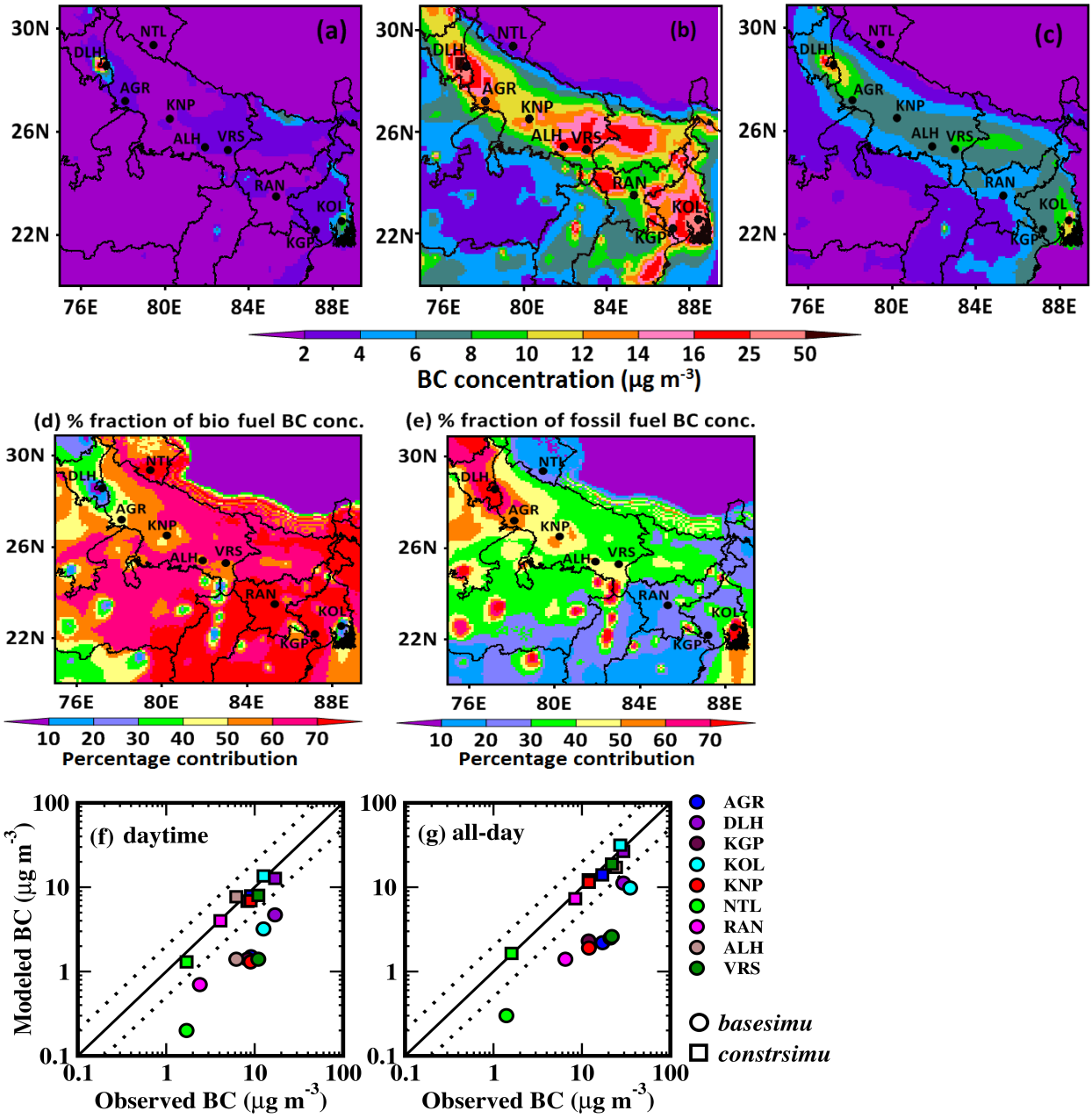

Figure 2. Spatial distribution of the simulated BC surface concentration ($\mu g\,m^{-3}$) averaged over the wintertime for (a) the *basesimu* experiment using baseline BC emission for all-day values and (b, c) the *constrsimu* experiment using constrained BC emission for (b) all-day and (c) daytime values. Fraction (%) of simulated BC concentration for *constrsimu* from (d) biofuel and (e) fossil-fuel emissions; (f–g) comparison of (f) daytime and (g) all-day wintertime mean of surface BC concentrations ($\mu g\,m^{-3}$) from simulations with measurements at stations over the IGP from available studies (refer to Table s1): Agra (Agr), Delhi (DEL), Kharagpur (KGP), Kolkata (KOL), Kanpur (KNP), Nainital (NTL), Ranchi (RAN), Allahabad/Prayagraj (ALH), Varanasi (VRS).

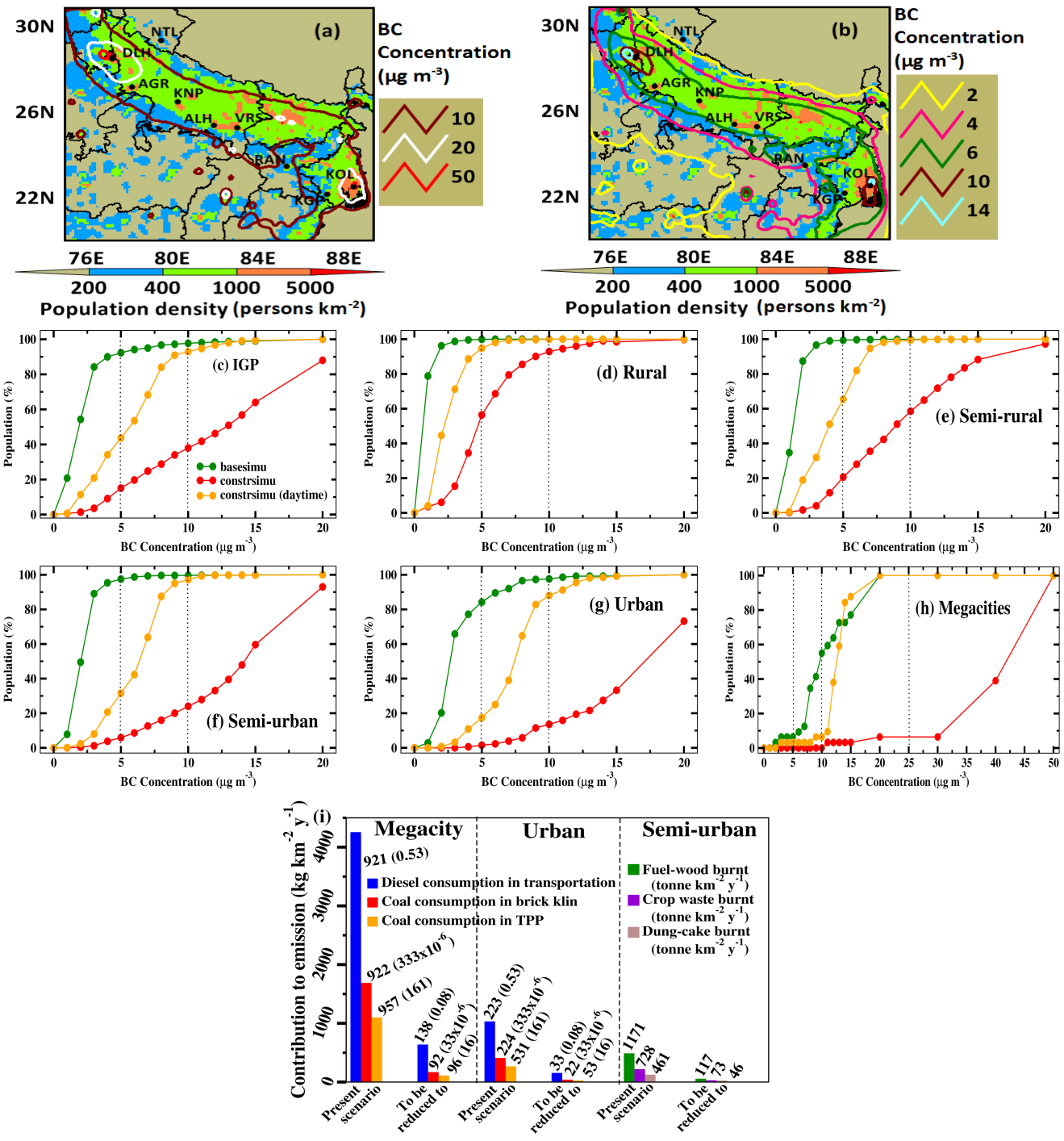

Figure 3. Spatial distribution of population density (number of inhabitants per km^2) overlaid with contours of BC concentration for wintertime (a) all-day mean of BC concentration and (b) daytime mean of BC concentration. Cumulative population exposure (%) to BC concentration from *constrsimu* and *basesimu* for the (c) entire IGP, and area-types of (d) rural (e) semi-rural, (f) semi-urban (g) urban and (h) megacity. (i) Domain-wise (megacity, urban, semi-urban) sustainable mitigation plan comprising of the amount of mitigation of emissions required ($x-axis$) from the present scenario (*constrsimu*) to the desired level (*basesimu*) for health-benefits from BC sanitary impacts through the corresponding reduction in fuel consumption for energy from identified combustion activity in a source sector. The $y-axis$ shows BC emission (with unit as kg km^{-2} yr^{-1}) arising from fuel consumption for energy (given as number on bars with unit as tonne km^{-2} yr^{-1}. The number inside the bracket shown on bars represent tonne yr^{-1} per heavy vehicle for diesel consumption, tonne yr^{-1} per 1000 bricks produced for coal consumption in brick kiln industry, tonne yr^{-1} per unit MW of electricity for coal consumption in TPP). The fuel consumption shown corresponds to the one which needs reduction on priority for health benefits to the population corresponding to an area-type.

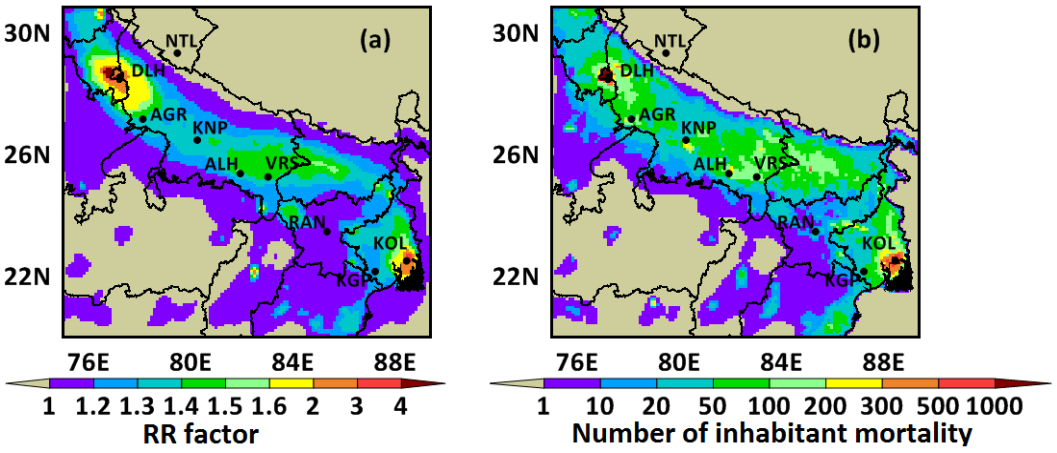

Figure 4. Spatial distribution (10×10 km^2 resolution) of health impact functions to assess BC attributable sanitary impacts for (a) Relative Risk factor, and (b) cardiovascular diseases mortality attributed to the wintertime BC exposure (CVM_{BC}^{WIN}, shown as number of inhabitants mortality per gridmesh on color scale).

Figures

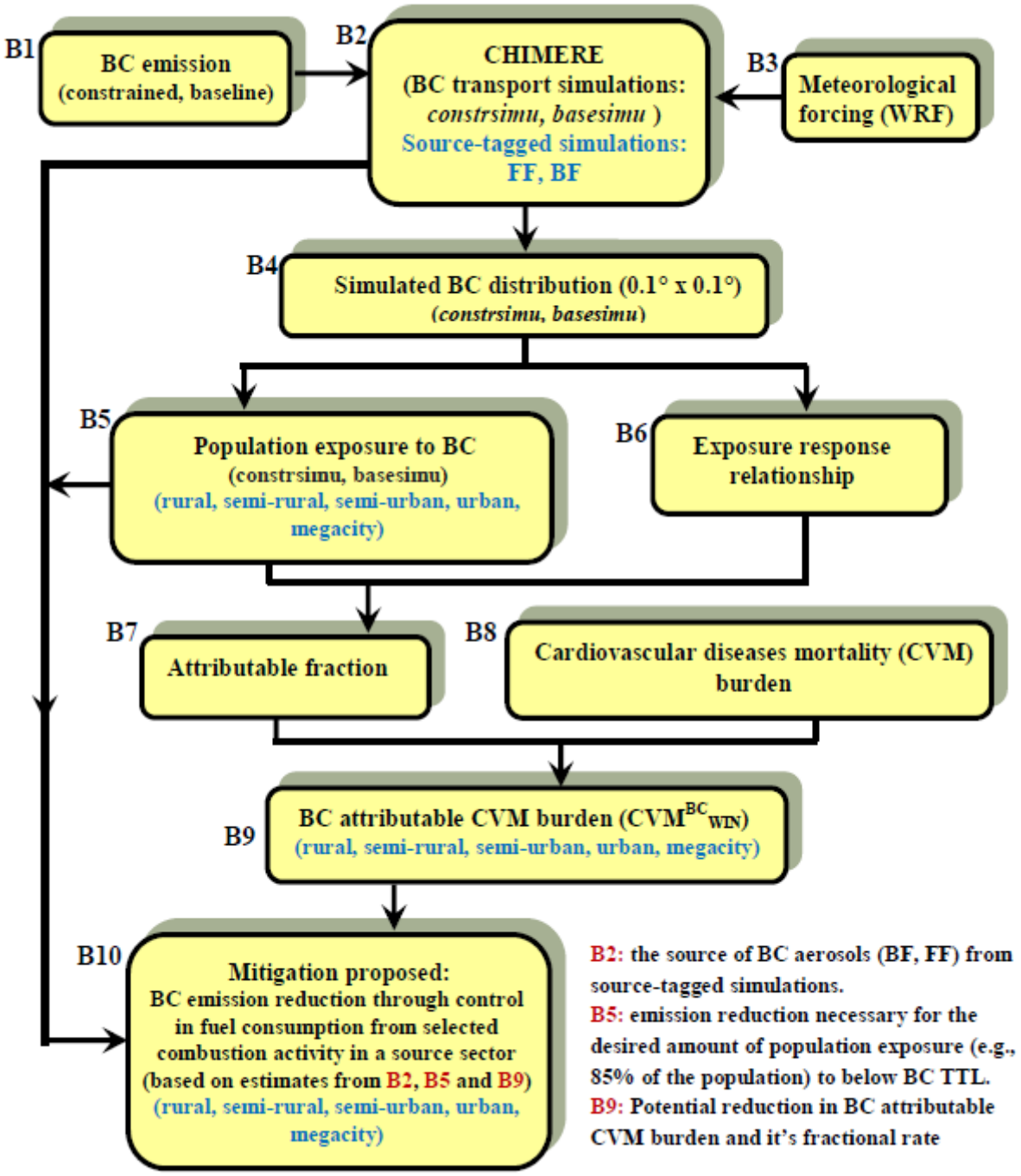

Figure 1

Flowsheet of conceptual plan to estimate the magnitude of BC attributable sanitary impacts and targeting sustainable BC emission reduction for health-benefits. The various blocks in the flowsheet are enumerated as B1, B2, B3...B10.

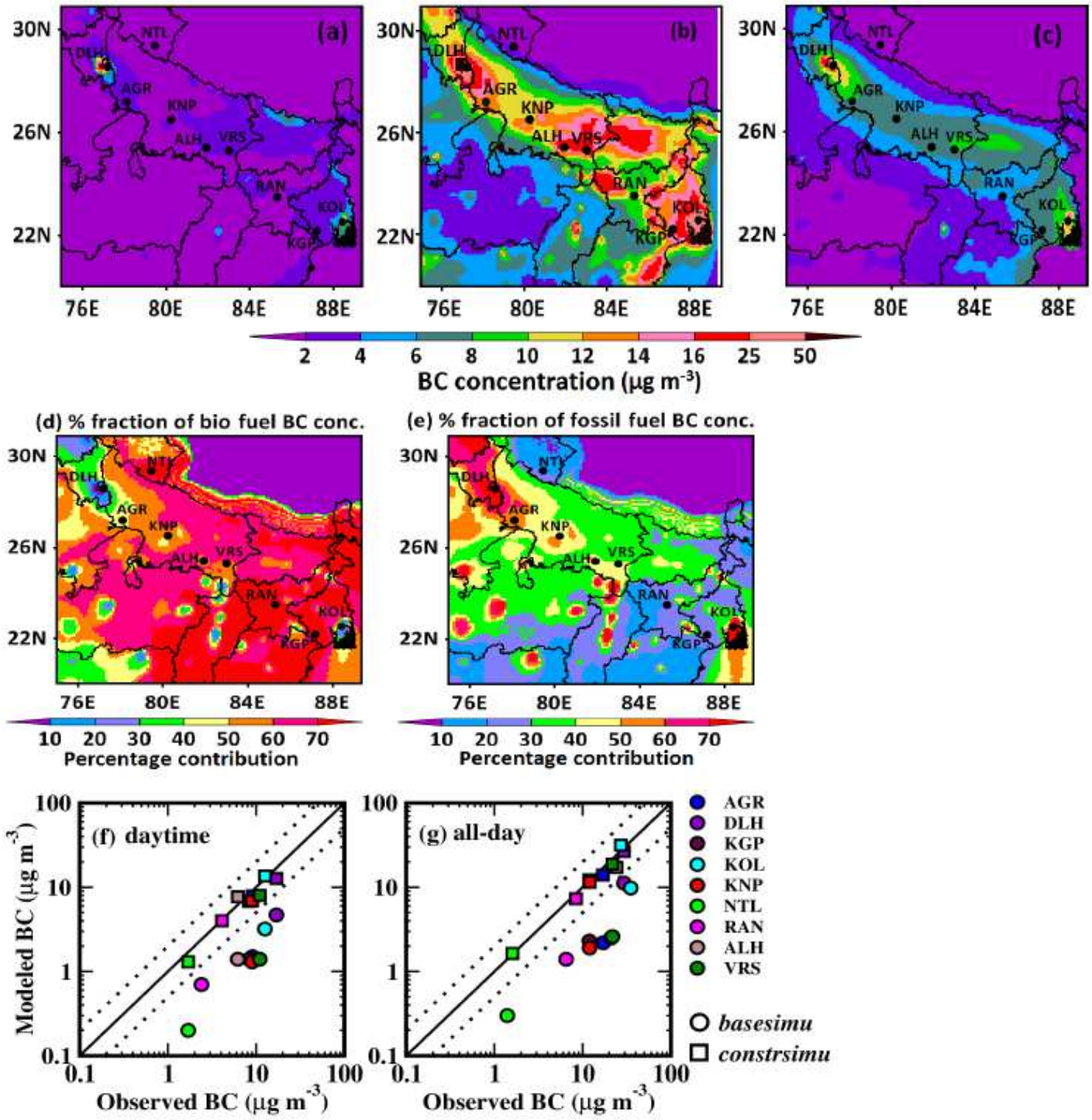

Figure 2

Spatial distribution of the simulated BC surface concentration (μgm−3) averaged over the wintertime for (a) the basesimu experiment using baseline BC emission for all-day values and (b, c) the constrsimu experiment using constrained BC emission for (b) all-day and (c) daytime values. Fraction (%) of simulated BC concentration for constrsimu from (d) biofuel and (e) fossil-fuel emissions; (f–g) comparison of (f) daytime and (g) all-day wintertime mean of surface BC concentrations (μgm−3) from simulations with measurements at stations over the IGP from available studies (refer to Table s1): Agra

(Agr), Delhi (DEL), Kharagpur (KGP), Kolkata (KOL), Kanpur (KNP), Nainital (NTL), Ranchi (RAN), Allahabad/Prayagraj (ALH), Varanasi (VRS).

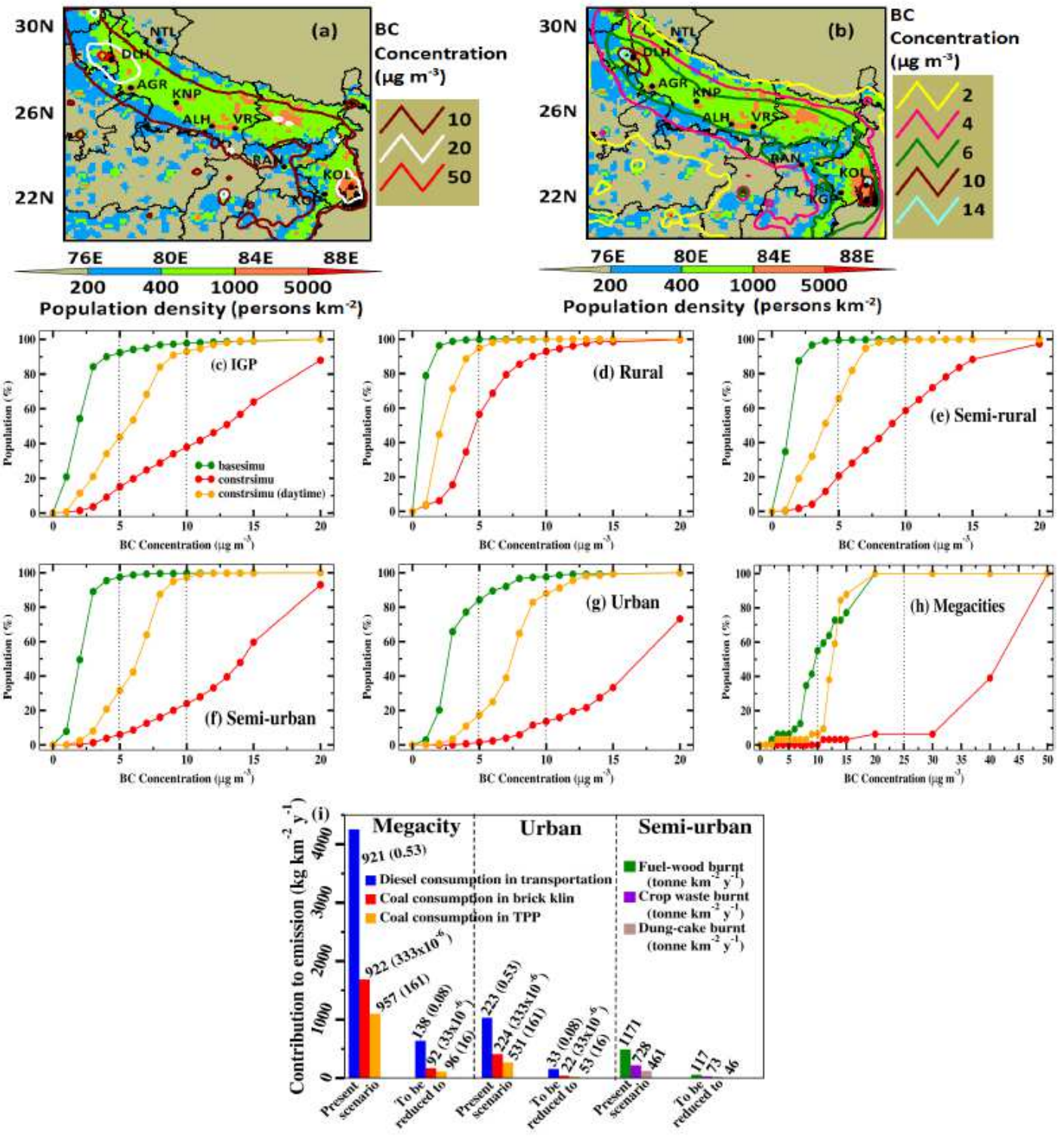

Figure 3

Spatial distribution of population density (number of inhabitants per km2) overlaid with contours of BC concentration for wintertime (a) all-day mean of BC concentration and (b) daytime mean of BC concentration. Cumulative population exposure (%) to BC concentration from constrsimu and basesimu

for the (c) entire IGP, and area-types of (d) rural (e) semi-rural, (f) semi-urban (g) urban and (h) megacity. (i) Domain-wise (megacity, urban, semi-urban) sustainable mitigation plan comprising of the amount of mitigation of emissions required (x−axis) from the present scenario (constrsimu) to the desired level (basesimu) for health-benefits from BC sanitary impacts through the corresponding reduction in fuel consumption for energy from identified combustion activity in a source sector. The y−axis shows BC emission (with unit as kg km−2 yr−1) arising from fuel consumption for energy (given as number on bars with unit as tonne km−2 yr−1. The number inside the bracket shown on bars represent tonne yr−1 per heavy vehicle for diesel consumption, tonne yr−1 per 1000 bricks produced for coal consumption in brick kiln industry, tonne yr−1 per unit MW of electricity for coal consumption in TPP). The fuel consumption shown corresponds to the one which needs reduction on priority for health benefits to the population corresponding to an area-type.

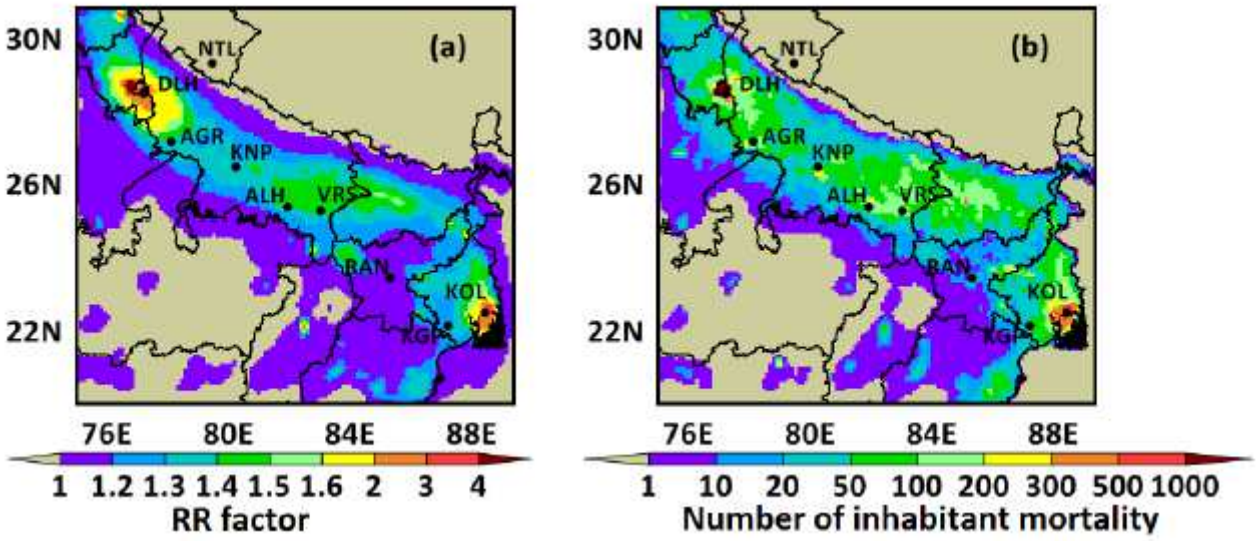

Figure 4

Spatial distribution (10 × 10 km2 resolution) of health impact functions to assess BC attributable sanitary impacts for (a) Relative Risk factor, and (b) cardiovascular diseases mortality attributed to the wintertime BC exposure (CVMWIN BC , shown as number of inhabitants mortality per gridmesh on color scale).

Supplementary Files

This is a list of supplementary files associated with this preprint. Click to download.

- supplementBCHealthimpact.pdf